THE JOURNAL OF BIOLOGICAL CHEMISTRY
Vol. 271, No. 46, Issue of November 15, pp. 28757–28765, 1996
Printed in U.S.A.

Fusogenic Properties of the C-terminal Domain of the Alzheimer β-Amyloid Peptide*

(Received for publication, March 25, 1996, and in revised form, July 18, 1996)

Thierry Pillot‡§, Marc Goethals¶, Berlinda Vanloo‡, Corinne Talussot‡, Robert Brasseur‖, Joel Vandekerckhove¶, Maryvonne Rosseneu‡, and Laurence Lins‖**

From the ‡Laboratory for Lipoprotein Chemistry and the ¶Flanders Interuniversity Institute for Biotechnology, Department of Biochemistry, Faculty of Medicine, University Gent, B-9000 Gent, Belgium and the ‖Centre de Biophysique Moléculaire Numérique, Faculté des Sciences Agronomiques de Gembloux, Gembloux, Belgium

A series of natural peptides and mutants, derived from the Alzheimer β-amyloid peptide, was synthesized, and the potential of these peptides to induce fusion of unilamellar lipid vesicles was investigated. These peptide domains were identified by computer modeling and correspond to respectively the C-terminal (*e.g.* residues 29–40 and 29–42) and a central domain (13–28) of the β-amyloid peptide. The C-terminal peptides are predicted to insert in an oblique way into a lipid membrane through their N-terminal end, while the mutants are either parallel or perpendicular to the lipid bilayer. Peptide-induced vesicle fusion was demonstrated by several techniques, including lipid-mixing and core-mixing assays using pyrene-labeled vesicles. The effect of peptide elongation toward the N-terminal end of the entire β-amyloid peptide was also investigated. Peptides corresponding to residues 22–42 and 12–42 were tested using the same techniques. Both the 29–40 and 29–42 β-amyloid peptides were able to induce fusion of unilamellar lipid vesicles and calcein leakage, and the amyloid 29–42 peptide was the most potent fusogenic peptide. Neither the two mutants or the 13–28 β-amyloid peptide had any fusogenic activity. Circular dichroism measurements showed an increase of the α-helical content of the two C-terminal peptides at increasing concentrations of trifluoroethanol, which was accompanied by an increase of the fusogenic potential of the peptides. Our data suggest that the α-helical content and the angle of insertion of the peptide into a lipid bilayer are critical for the fusogenic activity of the C-terminal domain of the amyloid peptide. The differences observed between the fusogenic capacity of the amyloid 29–40 and 29–42 peptides might result from differences in the degree of penetration of the peptides into the membrane and the resulting membrane destabilization. The longer peptides, residues 22–42 and 12–42, had decreased, but significant, fusogenic properties associated with perturbation of the membrane permeability. These data suggest that the fusogenic properties of the C-terminal domain of the β-amyloid peptide might contribute to the cytotoxicity of the peptide by destabilizing the cell membrane.

The amyloid peptide (Aβ),[1] a 39–43-residue peptide, is a normal 4-kDa derivative of a large transmembrane glycoprotein, the amyloid β precursor protein. The Aβ peptide is found in an aggregated, poorly soluble form in extracellular amyloid deposition in the brains and leptomeniges of patients with Alzheimer's disease (1). In contrast, it occurs in a soluble form in several biological fluids, including the cerebrospinal fluid, where it is produced by glial cells and neurons and where it circulates at nanomolar concentrations (2). The mechanism by which Aβ causes cell death and exerts its cytotoxicity effect remains unclear, and controversies still exist concerning the cytotoxic action of Aβ on neuronal cells. A number of *in vitro* studies with the synthetic Aβ peptide have shown that this peptide aggregates easily and forms amyloid fibrils similar to that found in the brain of patients with Alzheimer's disease (3–5). Recent observations have demonstrated that the C-terminal domain (amino acids 34–42) of Aβ is critical for amyloid aggregation and fibril formation (6).

Aggregated Aβ has been shown to be cytotoxic for cultured neurones, whereas nonaggregated peptide showed less cytotoxic effects (7–9). Arispe *et al.* (10, 11) have found that amyloid peptides were able to form calcium channels in bilayer membranes and other studies have suggested that the amyloid 1–40 and 1–42 peptides increased the intraneuronal free calcium concentration (12, 13). Moreover, recent reports have demonstrated a cytotoxic effect of Aβ, at relatively high doses (10–40 μM) on neuronal cells via an oxidative mechanism, which was not mediated by a receptor pathway (14, 15). Altogether, these data suggest a direct perturbation of cell membranes by the amyloid peptide. The mode of interaction of the peptide with the membrane has not been elucidated yet, and it is not clear whether aggregated Aβ can directly affect the cell membrane permeability or whether it enhances the membrane susceptibility to further injuries.

Membrane destabilization, due to the tilted penetration of fusion peptides into cellular membranes, is induced by a variety of peptides (16, 17). These hydrophobic peptides penetrate the lipid bilayer at an angle of 45–50°, due to the hydrophobicity gradient along their sequence (18, 19). Computer modeling of the β-amyloid peptide showed that the C-terminal domain of Aβ (*e.g.* amino acids 29–40 or 29–42) has properties similar to those of the fusion peptide of viral proteins (20). We therefore investigated the fusogenic properties of the C-terminal domain of amyloid peptide and report in this paper, that both the

* This work was supported in part by Grant G006196 from the Belgian National Funds for Scientific Research and by BioMed2 Program Grant CT 898.96. The costs of publication of this article were defrayed in part by the payment of page charges. This article must therefore be hereby marked "*advertisement*" in accordance with 18 U.S.C. Section 1734 solely to indicate this fact.

§ Recipient from a grant of the "Association Française pour la Recherche Thérapeutique."

** To whom correspondence should be addressed: Laboratory for Lipoprotein Chemistry, University Gent, Hospitaalstraat 13, B9000 Gent, Belgium. Tel.: 32-9-224-02-24; Fax: 32-9-225-34-89.

[1] The abbreviations used are: Aβ, β-amyloid peptide; SUVs, small unilamellar vesicles; LUVs, large unilamellar vesicles; SIV, Simian immunodeficiency virus; TFE, 2,2,2-trifluoroethanol; PE, L-α-phosphatidylethanolamine; PS, L-α-phosphatidyl-L-serine; PC, L-α-phosphatidylcholine; SM, sphingomyelin; Pyr-PC, 1-palmitoyl-2-pyrene(14)-phosphatidylcholine; E/M, the pyrene excimer/monomer ratio.

amyloid 29–40 and amyloid 29–42 peptides are able to cause fusion of unilamellar lipid vesicles with concomitant perturbation of membrane permeability as monitored by calcein leakage and that the amyloid 29–42 peptide is the most fusogenic. The α-helical structure and the obliquity of the peptides seem critical for their interaction with a lipid bilayer and for their fusogenic activity. The longer amyloid peptide, Aβ-(22–42) and Aβ-(12–42), had decreased but significative fusogenic activity, also associated with calcein release from the vesicles. This suggests that penetration of residues 29–42 into the membrane is hampered by N-terminal residues. Our results propose an alternative mechanism for the amyloid peptide cytotoxicity through a direct perturbation of the cellular plasma membrane similar to that induced by viral fusion peptides. The penetration of the cell membrane by the peptide at a tilted angle causes membrane perturbation and further cell damages.

EXPERIMENTAL PROCEDURES

Materials—L-α-Phosphatidylethanolamine (PE) from egg yolk, L-α-phosphatidyl-L-serine (PS) from bovine brain, L-α-phosphatidylcholine (PC) from egg yolk, free cholesterol, and bovine serum albumin were purchased from Sigma. Bovine sphingomyelin (SM) was from Matreya Inc. 1-Palmitoyl-2-pyrene-(14)-phosphatidylcholine (Pyr-PC) was a kind gift from P. Somerharju (University of Helsinki, Helsinki, Finland). All reagents for peptide synthesis and sequencing were purchased from Applied Biosystems. The trifluoroethanol (TFE) and hexafluoro-2-propanol used for sample preparation were of the highest grade from Sigma. 2′,7′-{Bis(carboxymethyl)aminomethyl} fluorescein (calcein) was from Molecular Probes.

Synthesis and Purification of Peptides—Peptides were synthesized by the standard Fmoc (*N*-(9-fluorenyl)methoxycarbonyl) solid-phase method, on an Applied Biosystems model 431A peptide synthesizer (21). The peptide-resin conjugate was cleaved with trifluoroacetic acid, and the peptide was precipitated with tributylmethyl ether and recovered by centrifugation at 2000 × *g*. The residue was dried for 2 h in a Speedvac concentrator (Savant Instruments, Farmingdale, NY). The peptides (20–40 mg) were resuspended in acetonitril/water (80/10, v/v) to get rid of all scavengers molecules and the insoluble peptide was recovered by centrifugation. The washing step with water was repeated 10 times. The purity and correct sequences of all peptides were verified by electron spray ionization mass spectrometry using a Fisons/VG Platform (Manchester, United Kingdom) mass.

Molecular Modeling of Peptides by Energy Minimization—Modelization of all peptides was carried out as described previously (16), and the method used is that applied to the study of polypeptide conformation (22). The method used to predict conformational structure of the peptides accounted for the contribution of the lipid-water interface, the concomitant variation of the dielectric constant, and the transfer energy of atoms from a hydrophobic to hydrophilic environment (23). The structure, mode of insertion, and orientation of the peptides were studied in a dipalmitoylphosphatidylcholine monolayer. In this model, the interaction energy (sum of contributions from Van der Waals energy interactions, torsional potential energy, electrostatic interactions, and transfer energy between peptide and dipalmitoylphosphatidylcholine in the monolayer) was calculated and minimized until the lowest energy state of the entire aggregate was reached. All calculations were performed on an Olivetti CP486, by using PC-TAMMO+ (Theoretical Analysis of Molecular Membrane Organization) and PC-PROT+ (Protein Plus Analysis) software. Graphs were drawn with the PC-MGM+ (Molecular Graphics Manipulation) program.

Circular Dichroism Measurements—To overcome problems of peptide solubility at high concentration, fresh peptide stock solutions (25 mg/ml) were prepared in hexafluoro-2-propanol, and peptides were further diluted in TFE. Circular dichroism spectra were obtained at 23 °C in a Jasco 710 spectropolarimeter calibrated with 0.1% (w/v) D-10-camphorsulfonic acid solution (24). Portions of peptide stock solutions were removed and diluted in a 10 mM sodium phosphate buffer, pH 7.4, containing different percentages of TFE. Nine spectra were recorded 20 min after the peptides were dissolved in the aqueous buffer/TFE solution at a final concentration of 0.1 mg/ml. The percentage of secondary structure were estimated by curve fitting on the entire ellipticity curve between 184 and 260 nm according to the variable selection procedure developed by Johnson (25).

Lipid Mixing Experiments—Small unilamellar vesicles (SUVs) were prepared from a mixture of PC/PE/PS/SM/cholesterol (10:5:7.5:7.5:16, w/w), when necessary in the presence of 2.5 mol% of Pyr-PC. The composition of the vesicles was selected to mimick that of rat neuronal membranes (26). All lipids were dissolved in chloroform at 10 mg/ml and dried under a stream of nitrogen. Pyr-PC was dissolved in chloroform/ethanol at a concentration of 2 μM. Dried mixed lipids were hydrated in a 10 mM Tris-HCl buffer, pH 8.0, containing 150 mM NaCl, 0.01% (w/v) Na-EDTA, and 1 mM NaN_3. The lipid suspension was sonicated at 23 °C, using a Branson sonifier, under nitrogen at 32 watts for 4 × 15 min. After sonication, the labeled and unlabeled vesicles were applied to a Sepharose CL-4B column. SUVs were separated from larger particles eluting in the void volume of the column. In order to obtain an homogenous preparation, only the top fractions of the SUV elution peak were collected and pooled. Phospholipid concentration was determined by an enzymatic assay (BioMérieux, Charbonnier les Bains, France). Large unilamellar vesicles (LUVs) were prepared from phospholipids as follows. Dry lipids were hydrated in buffer and dispersed by vortexing to produce large multilamellar vesicles. The lipid suspension was freeze-thawed five times and then extruded 10 times through two stacked 100-nm pore size polycarbonate filters in a pressure extruder (Lipex Biomembranes, Inc., Vancouver, Canada). The LUV and SUV preparations could be stored at 4 °C for at least 1 week, without significant size change of the vesicles during storage. Fusion of pyrene-labeled SUVs together with unlabeled vesicles, at a 1/4, w/w, ratio, was measured using a fluorescence probe dilution assay. The pyrene excimer/monomer intensity ratio was measured as a function of time after addition of increasing quantities of the peptides dissolved at a concentration of 1 mg/ml in either 50 or 20% (v/v) TFE. Fusion resulted in a decrease of the excimer intensity and a slight increase of the monomer fluorescence. Emission spectra were obtained on an Aminco SPF 500 spectrofluorimeter at 25 °C. The pyrene excimer/monomer (E/M) ratio was calculated from the excimer and monomer fluorescence intensity at 475 and 398 nm, respectively, with an excitation wavelength of 346 nm. The excitation and emission bandwidth were set at 2 and 5 nm, respectively. Under these conditions, unlabeled vesicles in the presence of the peptides gave no significant signal due to light scattering. All experiments were performed in a 10 mM Tris-HCl buffer, pH 8.0, containing 150 mM NaCl, and 0.1 g/liter Na-EDTA for a final volume of 500 μl. The final TFE concentration in the reaction mixture was less than 5%, and a correction was made for the effect of the solvent on the excimer/monomer ratio. The final peptide concentrations were in the range of 6.9 to 46 μM.

Visible Absorbance Measurements—The changes in the vesicle size distribution were monitored by visible absorbance measurements, as described previously (27). Aliquots of peptide stock solution (1 mg/ml in 50% TFE) were added to 15 μg of SUVs as for the fusion monitoring by fluorescence measurement. The absorbance at 405 nm was monitored in a function of time on a Uvikon 940 spectrophotometer.

Monitoring of Vesicle Size Increase by Gel Filtration—The ability of the labeled and unlabeled SUVs to undergo fusion was assessed by gel filtration on a Sepharose CL-4B column before and after the addition of the peptides. During gel filtration, the fluorescence emission intensity of Pyr-PC was continuously monitored.

Core-mixing Experiments—Vesicle fusion was also investigated by a core-mixing assay developed by Kendall and MacDonald (28). Lipid vesicles were prepared as described above except that the phospholipid mixture was prepared by hydrating 2 mg of phospholipids in 1.5 ml of a 10 mM Tris-HCl buffer, pH 8.0, containing 150 mM NaCl and 1 mM NaN_3 and containing calcein at 0.8 mM plus $CoCl_2$ at 1.0 mM or EDTA at 20 mM. Vesicles were then vigorously vortexed for 2 min and sonicated as described previously. Untrapped solutes were removed by two successive elutions on a Sephadex G-25 column with 10 mM Tris-HCl buffer, pH 8.0, containing 150 mM NaCl, and 1 mM NaN_3. The lipid concentrations of the liposome suspensions were determined by phosphorus analysis (29). In a standard experiment, calcein, Co^{2+}- and EDTA-containing vesicles were mixed at a 1:1 molar ratio in a 10 mM Tris-HCl buffer, pH 8.0, containing 150 mM NaCl and 1 mM NaN_3. Peptides from concentrated stock solutions were added at different concentrations and the calcein fluorescence was followed using an Aminco SPF 500 spectrofluorimeter, with excitation and emission wavelengths of 490 and 520 nm, respectively, and with excitation and emission slits of 5 nm. The maximum fluorescence yield was determined in the presence of 0.5% Triton X-100 and EDTA 10 mM. In some experiments, $CoCl_2$ at 0.4 mM chelated with 0.4 mM citrate were present in the reaction mixture to assess the leakage of encapsulated components. All experiments were performed under constant stirring at 25 °C in the fluorimeter cuvette.

Leakage of Liposome Contents—The leakage of liposome contents to the external medium was kinetically monitored by measuring the re-

TABLE I
Properties of the synthetic β-amyloid peptides

Mean hydrophobicity and hydrophobic moment were computed using the Eisenberg consensus scale (16). Underlined amino acids correspond to position changes compared to the Aβ-(29–42) wild-type peptide. The angle of insertion in a lipid bilayer was calculated according to 24.

Peptide	Peptide sequence	Predicted orientation	Angle of insertion	Mean hydrophobicity	Hydrophobic moment
Aβ-(13–28)	VHHQKLVFFAEDVGSNK			0.038	
Aβ-(29–40)	GAIIGLMVGGVV	Oblique	40°	0.874	0.12
Aβ-(29–42)	GAIIGLMVGGVVIA	Oblique	50°	0.890	0.04
Aβ-(29–42, 0°)	GAIIGLGVGMVVIA	Parallel	0°	0.890	0.04
Aβ-(29–42, 85°)	GVIIILMVGGAVGA	Perpendicular	85°	0.890	0.05
SIV	GVFVLGFLGFLA	Oblique	53°	0.930	0.09

lease of calcein trapped inside the vesicles (30). The SUVs were prepared as described previously except that dried lipids were rehydrated in a 10 mM Tris-HCl buffer, pH 8.0, containing 150 mM NaCl, 0.1 g/liter Na-EDTA, 1 mM NaN_3, and 40 mM calcein. At this concentration, fluorescence self-quenching occurs. Nontrapped calcein was removed by gel chromatography on Sephadex G-25. Vesicles were eluted with a 10 mM Tris-HCl buffer, pH 8.0, containing 150 mM NaCl, 0.1 g/liter Na-EDTA and 1 mM NaN_3. The lipid concentrations of the liposome suspensions were determined by phosphorus analysis (29). Calcein entrapped at a self-quenching concentration in SUVs increases in fluorescence when it leaks from inside the liposomes. Upon addition of the peptides from a 50% (v/v) TFE stock solution, the increase in calcein fluorescence was followed, using an Aminco SPF 500 spectrofluorimeter, with excitation and emission wavelengths of 490 and 520 nm, respectively, and with excitation and emission slits of 5 nm. 100% leakage was established by lysis of the vesicles with 0.5% (w/v) Triton X-100 (30). The percentage of calcein release is defined as: $\% F(t) = (I_t - I_0/I_{tot} - I_0) \times 100$, where I_0 = initial fluorescence, I_{tot} = total fluorescence observed after addition of Triton X-100, and I_t = fluorescence at time t. In our experimental conditions, in the absence of peptide, the spontaneous leakage rate was less than 1%/10 min. The volume of the reaction mixture was fixed at 500 μl. All experiments were with constant stirring at 25 °C.

RESULTS

The sequences and properties of the synthetic peptides representing different domains of the Alzheimer amyloid peptide (Aβ) are summarized in Table I. The central domain of the peptide Aβ is represented by the Aβ-(13–28) peptide, while peptides of the C-terminal domain of the Aβ peptide are designed as Aβ-(29–40) and Aβ-(29–42), respectively. In addition, two mutants of the A β-(29–42) peptide, named Aβ-(29–42, 0°) and Aβ-(29–42, 85°), were synthesized. These peptides have the same amino acid composition as the wild-type peptide, but their sequence was designed in order to change the angle of insertion of the peptides in a lipid bilayer. They are oriented at an angle of, respectively, 0 and 85° at a lipid/water interface, compared with an angle of 50° for the wild-type peptides (Table I). This obliquity is shared by viral fusion peptides, such as the Simian immunodeficiency virus fusogenic peptide (SIV) listed in Table I, whose properties have been extensively described (18). The amyloid C-terminal peptides are all highly hydrophobic, with an hydrophobicity close to that of a transmembrane peptide on the Eisenberg's scale (16). Compared with the C-terminal peptides, the 13–28 central peptide is much less hydrophobic and is not predicted to form a stable helix.

Computer Modeling of the Amyloid Peptides—In analogy with the calculations performed on the viral fusogenic peptides (20), the conformation of the β-amyloid peptides at a lipid/water interface was calculated by energy minimization (16). The most probable conformation of the peptides is illustrated in Fig. 1, showing the oblique orientation of the Aβ-(29–40) and Aβ-(29–42) peptides and of the SIV fusion peptide and the different orientation of the mutants. The oblique orientation of the wild-type peptides compared with the lipid bilayer is due to the concentration of the most hydrophobic residues at the N-terminal extremity of the peptide, thereby creating a N-C hydrophobicity gradient along the sequence. As described above, the peptides penetrate the phospholipid bilayer or insert into the lipid phase through their more hydrophobic N-terminal end and the 7–8 N-terminal residues insert into the lipid to destabilize the regular packing of the phospholipid acyl chains (Fig. 1).

Conformational Study of the Synthetic Amyloid Peptides—The secondary structure of the peptides was evaluated from their CD spectra in 20 and 50% TFE. In aqueous solution, Aβ-(29–40), Aβ-(29–42), Aβ-(29–42, 0°) and Aβ-(29–42, 85°) were poorly soluble and consisted essentially of a β-sheet structure, whereas the Aβ-(13–28) peptide exhibited largely random coil structure with a characteristic negative band at 198 nm (data not shown). Synthetic amyloid peptides required different concentrations of TFE to form α-helical structures. When the peptides were dissolved in 20% of TFE, Aβ-(13–28) displayed α-helix-forming propensities, and Aβ-(29–40) presented a mixture of α-helix and β-sheet structures (Fig. 2). On the contrary, 20% TFE was not sufficient to induce α-helix formation of the Aβ-(29–42), since the structure of this peptide consisted for 79% of β-sheet, with a characteristic negative band at 220 nm. As shown in Fig. 2, in the presence of 50% TFE, α-helical structures were formed with characteristic negative bands at 208 and 222 nm and a positive band at 192 nm. 50% of TFE promoted the formation of α-helix at a different extent for the three peptides, since the calculated α-helical content for Aβ-(13–28), Aβ-(29–40), and Aβ-(29–42) was, respectively, 25, 29, and 35%. These results suggest that the shorter Aβ-(29–40) peptide forms an α-helix more easily than the Aβ-(29–42). Under the same conditions, the Aβ-(29–42, 0°) mutant was 5 and 30% α-helical in 20 and 50% TFE, respectively, while the α-helical content of the Aβ-(29–42, 85°) mutant amounted to 1 and 39% in the same solvents (data not shown), suggesting that the amino acid sequence of the peptides is critical for the formation of stable α-helical structures.

Lipid Mixing Induced by the Tilted Peptides—The induction of intervesicular lipid mixing by peptides, as a measure of their fusogenic activity, was tested with PC/PE/PS/SPH/cholesterol SUVs utilizing a probe dilution assay (27, 31). SUVs labeled with pyrene-lecithin were mixed with unlabeled vesicles, and the ratio of the excimer to monomer intensity of the pyrene probe was measured as a function of time. A decrease of the excimer intensity and an increase of the monomer intensity due to the dilution of the probe into the fused vesicles is a measure of the fusion. As shown in Fig. 3, among the six peptides tested, only Aβ-(29–40) and Aβ-(29–42) had fusogenic properties monitored by the decrease of the E/M ratio of mixed unlabeled and labeled SUVs. The Aβ-(13–28), Aβ-(29–42, 0°), and Aβ-(29–42, 85°) peptides had not fusogenic activity, as predicted from computer modeling and from the calculation of the peptide obliquity (Table I). In a control experiment, the SIV peptide, with structural characteristics similar to those of the C-terminal domain of the amyloid peptide, showed fusogenic activity, thus confirming the validity of

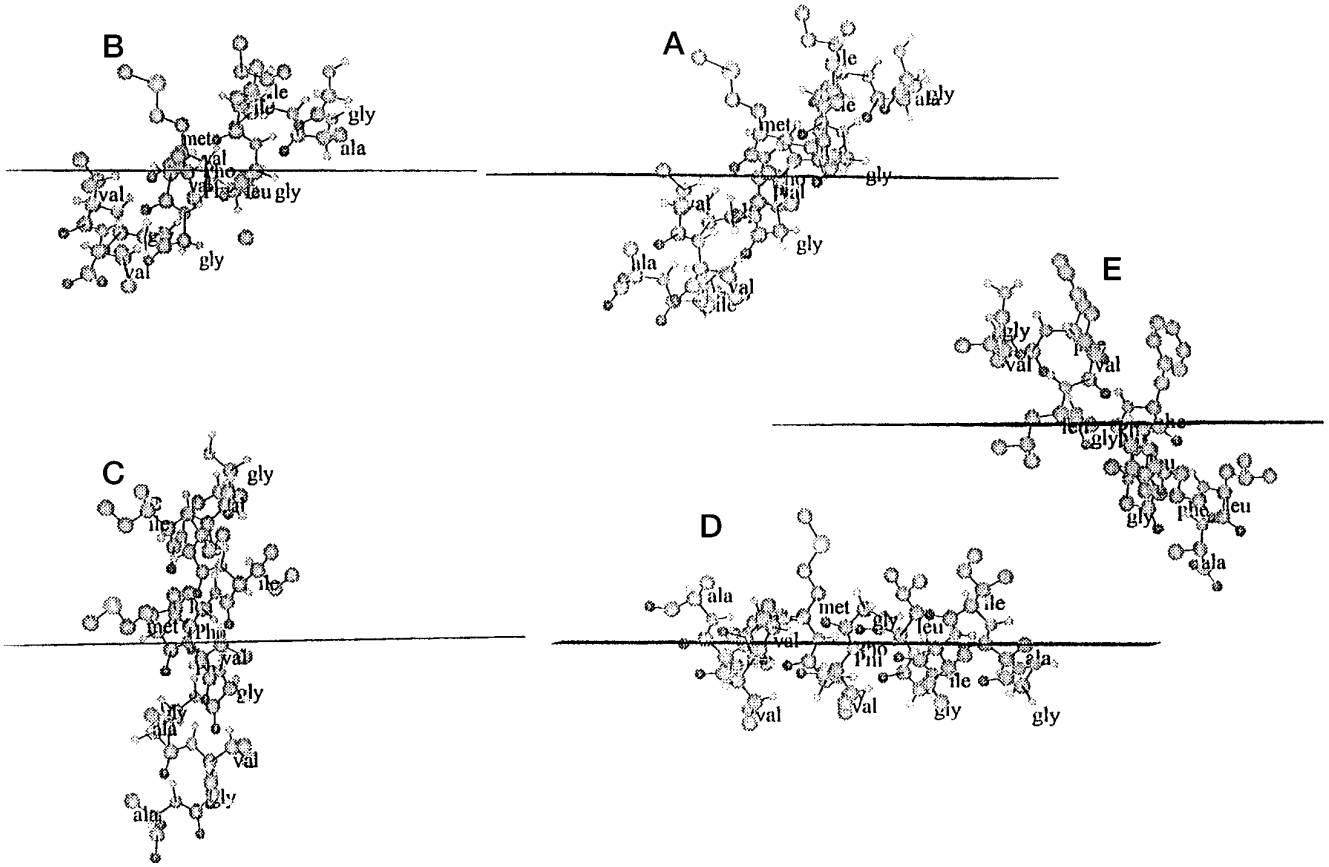

FIG. 1. **Computer modeling of the mode of insertion of the amyloid peptides within a lipid matrix.** For simplicity reasons, lipids were not drawn. The *horizontal line* represents the interface between the hydrophobic (upper) and the hydrophilic phase. The modelized peptides are as follows from *right* to *left*: *A*, Aβ-(29–42); *B*, Aβ-(29–40); *C*, Aβ-(29–42, 85°); *D*, Aβ-(29–42, 0°), and *E*, SIV.

the experimental approach (Fig. 3). Similar results were obtained using labeled and unlabeled LUV preparations to monitor lipid mixing induced by the amyloid and the SIV peptides (data not shown). The dependence of both the extent and kinetics of the lipid mixing process, on the peptides concentration, was examined. In separate experiments, increasing amounts of Aβ-(29–40) and Aβ-(29–42) peptides were added to a fixed amount of SUVs. The time course variation of the E/M ratio induced by adding various amounts of the two peptides showed that both peptides are able to cause lipid mixing, in a concentration-dependent manner. To compare the activity of the two peptides, the level of the E/M ratio decrease 10 min after the addition of the peptide was measured and is depicted on Fig. 4. Aβ-(29–42) is more active in inducing SUVs fusion than the Aβ-(29–40) peptide, as the Aβ-(29–42) peptide causes fusion more rapidly and to a higher extent than Aβ-(29–40). At 46 μM, the Aβ-(29–42) caused a 71.5% of E/M ratio decrease after 10 min of incubation with the vesicles, whereas at the same peptide concentration, the E/M ratio decreased of 59% when the Aβ-(29–40) peptide was mixed with the vesicles. Same results were obtained using PC/PE/cholesterol LUVs (data not shown). In control experiments, incubation of mixed labeled and unlabeled vesicles, in the absence of peptide or incubation of labeled vesicles alone with the Aβ-(29–40) or Aβ-(29–42) peptides, had no effect on the E/M ratio (data not shown). These results strongly suggest that the observed lipid mixing induced by the amyloid peptides is the result of intervesicular lipid mixing, as suggested by Morris *et al*. (31).

In order to assess the influence of the secondary structure of the peptides on their fusogenic activity, the peptides were diluted in 20 or 50% TFE and added to the SUV preparation (Fig. 5). Compared with the effect measured with peptides dissolved in 50% TFE, solubilizing the peptides in 20% TFE decreased intervesicular lipid mixing. As the percentage α-helical structure of the peptides is maximal in 50% TFE, as shown in Fig. 2, this suggests that the fusogenic properties of the peptides increase with their helical conformation. This effect is more pronounced for the Aβ-(29–42) peptide whose α-helical content increases most between 20 and 50% TFE.

Visible Absorbance Studies and Gel Filtration—Changes in vesicles size distribution resulting from fusion can be monitored by following the absorbance of the SUV preparation (27). The changes of absorbance at 405 nm as a function of time after addition of the peptides to SUV suspension are plotted in Fig. 6, *A* and *B*. The data show that, at all concentrations tested, Aβ-(29–40) and Aβ-(29–42) induce an increase of vesicle size. The initial rate and the total amplitude of the absorbance increase are highest for the Aβ-(29–42) peptide, and these differences are more pronounced at higher peptide concentrations (46 μM). At this peptide concentration, the absorbance measured after addition of Aβ-(29–42) reached its final level within 4–5 min, whereas the Aβ-(29–40) peptide initially induced a moderate increase of absorbance followed by a slower increase. These data are in agreement with those obtained by fluorescence measurements (Figs. 3 and 4). The SIV fusion peptide, at a concentration of 13.8 μM, had a similar effect on vesicular size, whereas the Aβ-(29–42, 0°) and Aβ-(29–42, 80°) peptides had no effect (Fig. 6*C*). To confirm that the turbidity increase and the intervesicular lipid mixing resulted of membrane fusion, the increase of vesicle size induced by the amyloid peptides was also monitored by gel filtration on a Sepharose CL-4B column. Fig. 7 shows that incubation of an homogenous population of pyrene-labeled vesicles with unlabeled vesicles, in the presence of the Aβ-(29–40) and Aβ-(29–42) peptides,

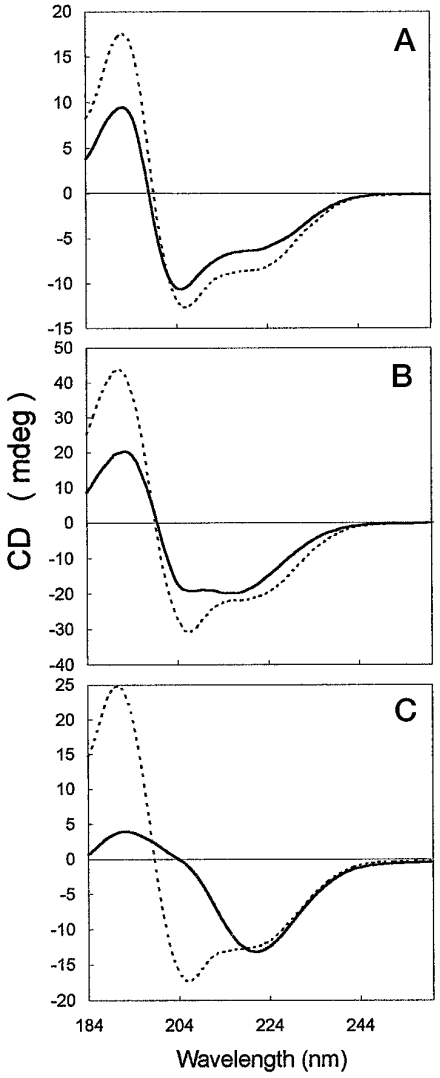

FIG. 2. **Circular dichroism spectra of synthetic amyloid peptides at 23 °C.** Peptides were dissolved, at 0.1 mg/ml, 20 min before measurements in a 10 mM phosphate, pH 7.4 buffer, containing 20% (*solid line*) and 50% (*dashed line*) of TFE. *A*, Aβ-(13–28); *B*, Aβ-(29–40); and *C*, Aβ-(29–42).

significantly increases the size of the particles. The pyrene intensity is maximum within the void volume of the Sepharose CL-4B column. By comparison, the mixture eluted as a major peak within the separation volume of the column when no peptide or the Aβ-(13–28) peptide was added (Fig. 7).

Lipid Mixing Induced by the Aβ-(22–42) and Aβ-(12–42) Peptides—Computer modelization of the amyloid peptide carried out on the C-terminal domain of the β-amyloid peptide predicted that it inserts into the lipid bilayer via its N-terminal residues (Fig. 1). In order to investigate the effect of the elongation of the peptide at its N-terminal end, we synthesized longer peptides spanning residues 22–42 and 12–42, Aβ-(22–42) and Aβ-(12–42) peptides, respectively. As shown in Fig. 8, both peptides were able still to induce fusion of SUVs measured by lipid-mixing assay within the same concentration range as described above. The same results were obtained using labeled and unlabeled LUVs (data not shown). When the peptides were incubated at 46 μM with a mixture of labeled and unlabeled SUVs, the Aβ-(22–42) peptide induced a E/M ratio decrease of about 48% and the Aβ-(12–42) peptide a decrease of 37%, compared with 72% for the Aβ-(29–42) peptide. Incubation of the peptides with pyrene-labeled vesicles in the absence of unlabeled vesicles showed no decrease of the pyrene excimer/monomer ratio, suggesting that the observed fusion was due to membrane intermixing and was not due to exchange of pyrene-labeled phospholipids facilitated by simple vesicle aggregation (data not shown). These results suggest that the addition of N-terminal residues of the Aβ peptide has only limited effects on the interaction of the C-terminal fusogenic peptide with a lipid bilayer and that this tilted peptide is still able to induce fusion within the longer Aβ peptides.

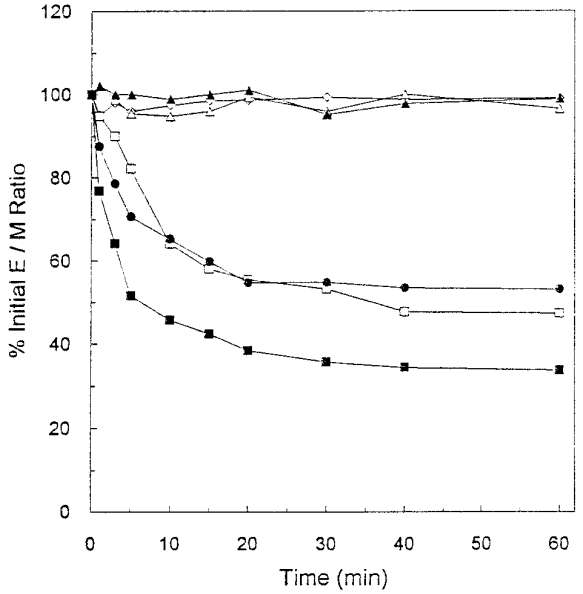

FIG. 3. **Time course of lipid mixing of PC/PE/PS/SM/cholesterol SUVs induced by 13.8 μM amounts of different peptides.** Peptide aliquots were added to a mixture of labeled SUVs (3 μg of phospholipid) containing 2.5 mol% of Pyr-PC and of unlabeled SUVs (12 μg of phospholipid) in a 10 mM Tris-HCl, pH 8.0 buffer, containing 150 mM NaCl, 1 mM NaN_3, and 0.01 g/liter Na-EDTA. The Pyr-PC excimer/monomer ratio was monitored at room temperature and is plotted as a percentage of the initial value *versus* time. The different peptides used in this experiment were: Aβ-(13–28) (◇), Aβ-(29–40) (□), Aβ-(29–42) (■), Aβ-(29–42, 0°) (△), Aβ-(29–42, 85°) (▲), SIV (●).

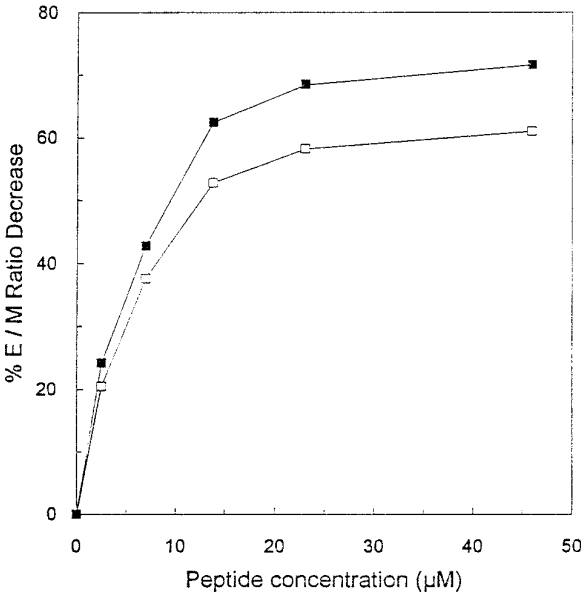

FIG. 4. **Influence of the peptide concentration on the extent of lipid mixing of PC/PE/PS/SM/cholesterol SUVs induced by the Aβ-(29–40) (■) and Aβ-(29–42) (□) peptides.** Percentages of E/M ratio decrease was plotted *versus* peptide concentration, after 10-min incubation of SUVs and peptide.

Core Mixing Induced by the Synthetic Amyloid Peptides—In

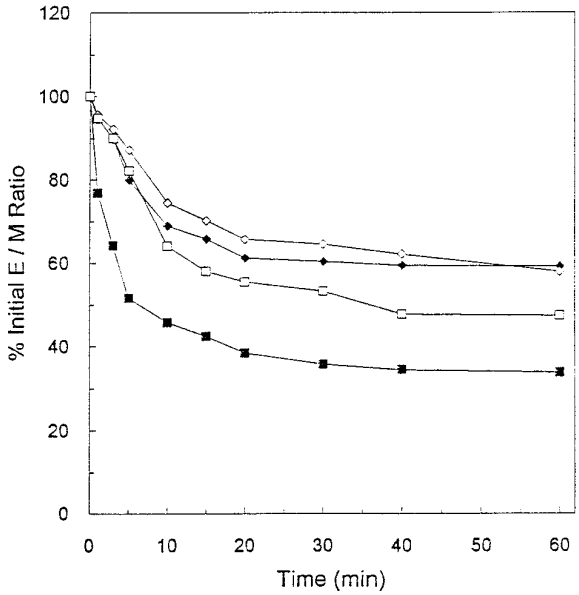

FIG. 5. **Influence of the peptide secondary structure on the time course of lipid mixing of PC/PE/PS/SM/cholesterol SUVs induced by Aβ-(29–40) and Aβ-(29–42) peptides.** Peptides were dissolved in a 10 mM Tris-HCl, pH 8.0 buffer, containing 150 mM NaCl, 1 mM NaN_3, 0.01 g/liter Na-EDTA, and 20 or 50% of TFE. Peptide aliquots were added to a mixture of labeled SUVs (3 μg of phospholipid) containing 2.5 mol% of Pyr-PC and of unlabeled SUVs (12 μg of phospholipid). The Pyr-PC excimer/monomer ratio was monitored at room temperature and is plotted as a percentage of the initial value *versus* time. Conditions for peptide solubilization were Aβ-(29–40) in 20% TFE (◇), Aβ-(29–40) in 50% TFE (□), Aβ-(29–42) in 20% TFE (♦), and Aβ-(29–42) in 50% TFE (■).

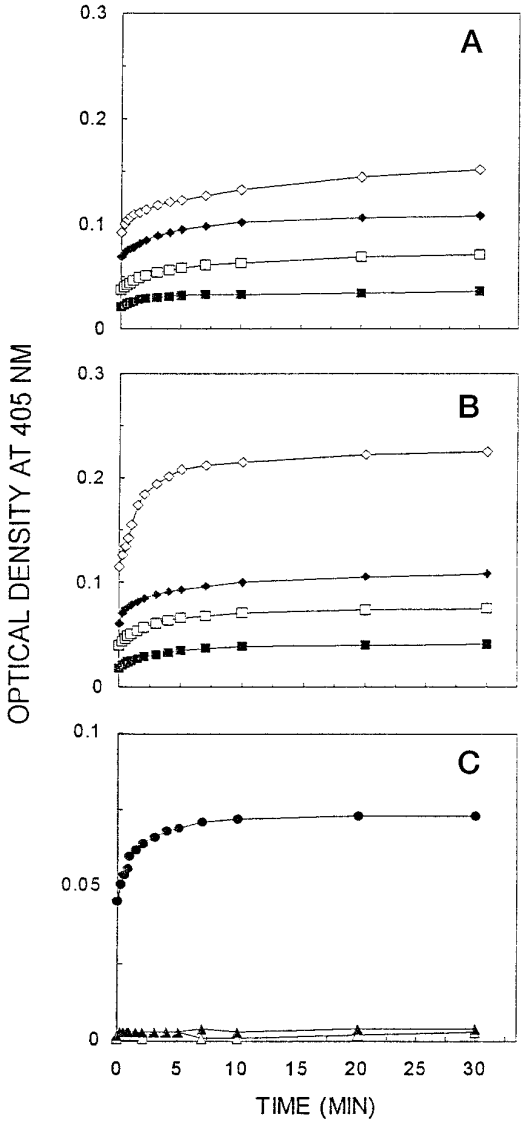

FIG. 6. **Monitoring of vesicle fusion and/or aggregation by measurement of the absorbance at 405 nm of lipid vesicles mixed with synthetic amyloid peptides.** Peptides were dissolved at 1 mg/ml in 50% TFE, and peptide aliquots were added to a mixture of labeled SUVs (3 μg of phospholipid) containing 2.5 mol% of Pyr-PC and of unlabeled SUVs (12 μg of phospholipid) in a 10 mM Tris-HCl, pH 8.0 buffer, containing 150 mM NaCl, 1 mM NaN_3, and 0.01 g/liter Na-EDTA. The changes in absorbance at 405 nm are plotted *versus* time after the addition of the peptides: Aβ-(29–40) (*A*) and Aβ-(29–42) (*B*) at 6.9 μM (■), 13.8 μM (□), 23 μM (♦), and 46 μM (◇). *C*, Aβ-(29–42, 0°); (■), Aβ-(29–42, 85°) (□) and SIV (♦) peptide at 46 μM.

order to further document the fusogenic properties of the amyloid peptides previously monitored by the lipid-mixing assay and supported by visible absorbance measurements and gel filtration, experiments were carried out to demonstrate contents mixing of two vesicle populations labeled separately (28). When the amyloid peptides were added to a mixture of calcein and Co^{2+}- and EDTA-containing PC/PE/PS/SPH/cholesterol SUVs, an increase of the fluorescence was observed (data not shown). The observed increase in fluorescence due to increase concentration of free calcein, could be a consequence of EDTA-Co^{2+} complex formation occurring within the inner compartment of the fused vesicles. On the other hand, if leakage of the vesicle contents occurs, dilution and subsequent dissociation of calcein-Co^{2+} complex might take place. This would increase the emission intensity of the free calcein. Fluorescence due to leakage of vesicle contents can be eliminated by adding 0.4 mM Co^{2+} (chelated in a 1:1 molar ratio with citrate) in the outer phase. Fig. 9 illustrates the effect of increasing concentrations of the different amyloid peptides on the core mixing of calcein and Co^{2+}- and of EDTA-containing SUVs after 10 min of incubation in the presence of Co^{2+} in the external phase. The results show that both peptides can induce content mixing of the two populations of vesicles within the same concentration range as in the lipid mixing experiments. In agreement with the lipid-mixing assay, the Aβ-(29–42) peptide is the most fusogenic peptide as it induces a 23% increase of the calcein emission intensity at 46 μM, compared with 19% for the Aβ-(29–40) peptide. As described above, the longer peptides are still able to induced vesicle fusion monitored by a core-mixing assay. In control experiments, we demonstrated that neither the Aβ-(29–42, 0°), the Aβ-(29–42, 85°), or the Aβ-(12–28) peptides were able to cause significant content mixing of the two populations of vesicles (data not shown).

Peptide-induced Leakage of Liposomal Contents—Experiments from core-mixing assay suggested that concomitantly with membrane fusion, release of vesicle contents occurred in the presence of the amyloid peptides. To assess the leakage of vesicle contents due to the interaction with the synthetic amyloid peptide, we performed leakage measurement of encapsulated free calcein from SUVs. The addition of the C-terminal amyloid peptides to SUVs (15 μg of phospholipids) produced membrane destabilization as measured by the release of calcein from the vesicles. Fig. 10 illustrates the concentration-dependent release of calcein from SUVs, induced by the addition of the Aβ-(29–40), Aβ-(29–42), Aβ-(22–42), and Aβ-(11–42) peptides. Within this concentration range, the rate of calcein leakage was significant for all peptides. As shown in Fig. 10, after 10 min of incubation, the Aβ-(29–42) peptide was more active than the Aβ-(29–40) peptide, in agreement with the results from the lipid-mixing assay (Fig. 4) and consistent with

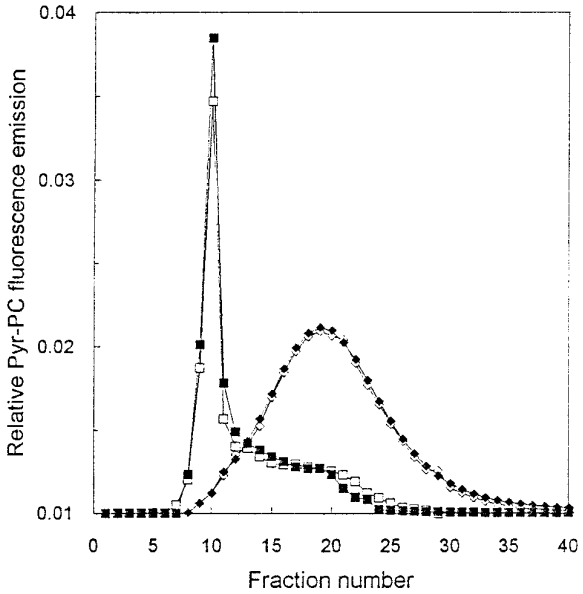

FIG. 7. **Monitoring of vesicle size by size-exclusion chromatography.** Peptides were dissolved at 1 mg/ml in 50% TFE, and peptide aliquots (13.8 μM) were added to a mixture of labeled SUVs (3 μg of phospholipid) containing 2.5 mol% of Pyr-PC and of unlabeled SUVs (12 μg of phospholipid). After 15-min incubation in the presence of Aβ-(13–28) (◇), Aβ-(29–40) (□), Aβ-(29–42) (■) peptides, or in the absence of peptide (◆), the lipid mixture was applied to a Sepharose CL-4B column, and the elution profile was recorded by monitoring the Pyr-PC fluorescence emission at 398 nm. The void volume of the Sepharose column corresponded to fraction number 9.

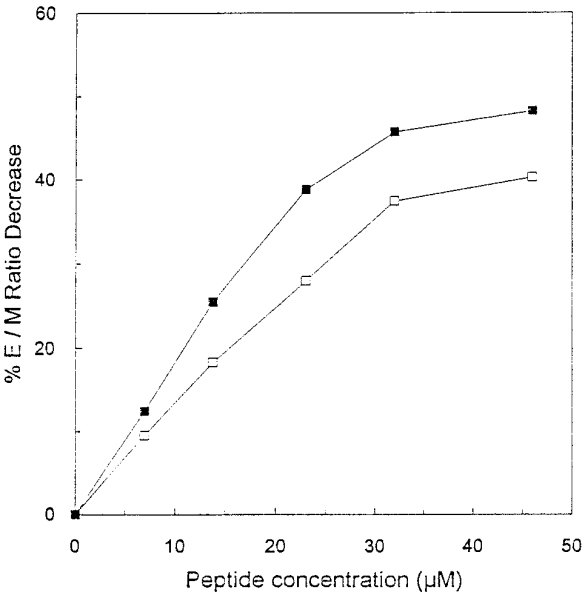

FIG. 8. **Lipid mixing of PC/PE/PS/SM/cholesterol SUVs induced by the Aβ-(22–42) (■) and Aβ-(12–42) (□) peptides.** Percentages of E/M ratio decrease was plotted *versus* peptide concentration, after 10-min incubation of SUVs and peptide.

the previously discussed differences in bilayer penetration (Fig. 1). In agreement with the results of the lipid- and core-mixing assays, the Aβ-(22–42) and the Aβ-(11–42) peptides were also able to perturb the membrane of the vesicles and to induce calcein release from the SUVs. In control experiments, we observed that the Aβ-(13–28) peptide caused a nonsignificant calcein release of 9.5 and 10.6% after 10 min of incubation at 23 and 46 μM, respectively (data not shown). Under the same experimental conditions, the Aβ-(29–42, 0°) and the Aβ-(29–42, 85°) peptides at 46 μM induced a calcein release of 19 and

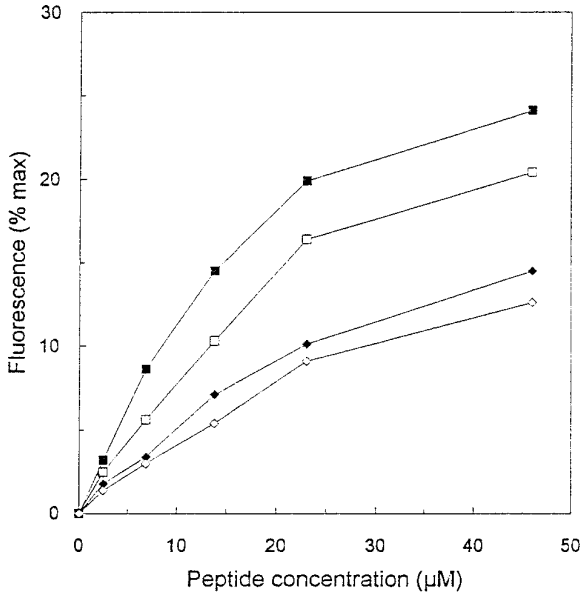

FIG. 9. **Mixing of liposomal contents induced by the β-amyloid peptides.** Peptides were dissolved at 1 mg/ml in 50% TFE, and peptide aliquots were added to a mixture of calcein and Co^{2+}- and of EDTA-containing SUVs (1:1 ratio, 15 μg of phospholipids) in a 10 mM Tris-HCl, pH 8.0 buffer, containing 150 mM NaCl, 1 mM NaN_3, and 0.4 mM Co^{2+} chelated with 0.4 mM citrate. Core mixing of the two populations of vesicles was followed as described under "Experimental Procedures," and the percentage of the maximum calcein fluorescence after 10-min incubation was plotted as a function of the peptide concentration. ■, Aβ-(29–42); □, Aβ-(29–40); ◆, Aβ-(22–42); and ◇, Aβ-(12–42). 100% of the calcein fluorescence was established by lysing the vesicles with Triton X-100 (0.5% w/v) in the presence of 10 mM EDTA.

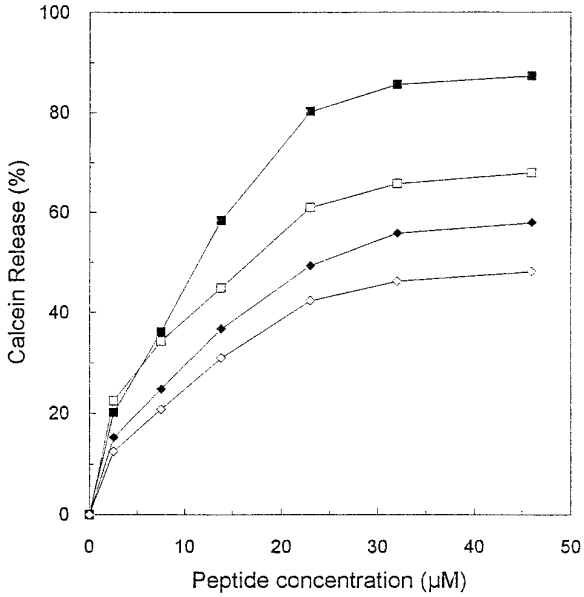

FIG. 10. **Leakage of liposomal contents induced by the β-amyloid peptides.** Peptides were dissolved at 1 mg/ml in 50% TFE, and peptide aliquots were added to calcein SUVs (15 μg phospholipids) in a 10 mM Tris-HCl, pH 8.0 buffer, containing 150 mM NaCl, 1 mM NaN_3, and 0.01 g/liter Na-EDTA. Calcein release from the vesicles was followed as described under "Experimental Procedures," and percentage of calcein release after 1 h of incubation with increased concentration of β-amyloid peptides was plotted as a function of the peptide concentration. (■), Aβ-(29–42); □, Aβ-(29–40); ◆, Aβ-(22–42); and ◇, Aβ-(12–42). 100% of leakage was established by lysing the vesicles with Triton X-100 (0.5% w/v).

23%, respectively (data not shown). We cannot rule out an aspecific interaction of these peptides with the SUVs due to their high hydrophobicity. This suggests however that the

tilted insertion of the peptides into the lipid enhanced the release of the encapsulated calcein. The limited effect of the Aβ-(13–28) peptide and of the Aβ-(29–42) mutant peptides suggests that the leakage of the liposomal content induced by the wild-type peptide, is specific. Altogether, these results suggest that the fusion of SUVs induced by the amyloid peptides is correlated to lipid bilayer destabilization via a direct interaction of the amyloid peptide with the lipid phase and that this process is mediated by the C-terminal end of the peptide (*e.g.* amino acids 29–42).

DISCUSSION

Several papers recently appeared concerning the structural characterization of either the entire β-amyloid peptide, or of some of its synthetic fragments, in relation to their aggregation properties (for review, see Ref. 2). Many studies have demonstrated that the Aβ peptide, as well as analogs, become toxic for cultured neuronal cells only when they form fibrillar aggregates (8, 9). This was observed for the 25–35 and 34–42 amyloid peptides, which are highly toxic for cells and are both able to form amyloid fibrils. Recent results from Lansbury *et al*. (6) proposed a model of the formation and structure of fibrils, where the amyloid 34–42 peptide plays a critical role in the stabilization and growth of these fibrils. However, these structural data could not provide with a mechanism for fibril formation or for the damages induced by the Aβ peptide to cell membranes and for its ability to kill neurons. Recent studies suggest that the amyloid peptide might be toxic for cultured neurons via an oxidative mechanism independent of a receptor interaction, suggesting a direct interaction of the peptide with the cell membrane (14). By analogy with other peptides, active on cell membranes, Aβ has an ordered amphiphilic nature, which could be in part responsible for its toxicity. Another amyloidogenic peptide, calcitonin, appears as an amphiphilic α-helix in solution. The cluster of positive charges localized on one side of the helix suggests that the hydrophilic part of the molecule remains at the cell surface while the hydrophobic part of the peptide can penetrate the plasma membrane (32). Similarly, the cytotoxic peptides, mastoparan and mellitin, are thought to insert into the membrane where they perturb several membrane-associated enzymes and signaling pathways (33, 34). Fusion of phospholipid membranes is thought to involved three steps: vesicle aggregation, membrane destabilization, and merging of membrane. Using computer modeling, we localized in the C-terminal domain of Aβ, a peptide with physico-chemical properties close to those of putative fusion peptide of several viral proteins (20). The obliquity and the high hydrophobicity of the 29–40 and 29–42 amino acids of Aβ are consistent with such potential fusogenic properties. Our *in vitro* data clearly indicate that these peptides are able to induce fusion of unilamellar lipid vesicles. The results from both the lipid-mixing and the core-mixing experiments (Figs. 4, 8, and 9), and the monitoring of vesicle size increase (Fig. 6 and 7) shows that the Aβ-(29–42) peptide is the more potent fusogenic peptide and that its fusogenic properties are closest to those of the SIV fusion peptide. By analogy with this peptide, the Aβ-(29–42) peptide may be a better fusogenic peptide, because it can insert deeper into the lipid bilayer than the Aβ-(29–40) peptide. Considering that in our lipid-mixing assay, the ratio of the fluorescence-labeled/unlabeled vesicles is 1:4, the above decrease in the surface density of the pyrene-labeled phospholipids is consistent with an amyloid peptide-induced fusion between the labeled and unlabeled SUVs, followed by lateral diffusion of the fluorescent probes in the plane of the newly enlarged membranes. Simple aggregation of the vesicles would not result in such a change of the pyrene excimer/monomer ratio (35). Moreover, fused vesicles could be resolved by gel filtration, and large and unspecific aggregation of the lipid vesicles was avoided during the time course of our experiments. When the fluorescence-labeled vesicles were mixed with the peptides in the absence of unlabeled vesicles, there was no change in the pyrene excimer/monomer ratio. This indicates that the effect observed above was not due to a simple exchange of pyrene-phospholipid between labeled vesicles and was not due to a change in the shape or in the radius of curvature of the vesicles. In the same way, mixing of labeled and unlabeled vesicles in the absence of peptide did not result in a decrease of the pyrene excimer/monomer ratio. Thus, the vesicles used were stable for at least 1 week at 4 °C, indicating that an apparent fusion resulting from vesicle instability can be discarded (30, 36). These results were further confirmed by core-mixing experiments (Fig. 9). Within the same concentration range used for the lipid-mixing assay, the four amyloid peptides tested were able to induce mixing of core contents of liposomes. In agreement with the data from the lipid-mixing assay, the Aβ-(29–42) was the most fusogenic peptide and the elongation of this peptide at its N-terminal end did not abolish the fusogenic properties of the C-terminal domain of the amyloid peptide.

This fusogenic activity is related both to the peptide concentration and to the α-helical content of the peptides (Figs. 4 and 5). Formation of an α-helical structure may promote easier association with the lipid bilayer and penetration of the peptide. Such observations have been described for other fusion peptides such as the N-terminal fusion peptide of the Sendai virus (27). These results are supported by experiments carried out with mutant Aβ-(29–42) peptides with the same hydrophobicity but a different orientation at a lipid/water interface and with the Aβ-(13–28) peptide, which is not fusogenic. These data stress the crucial effect of the obliquity and hydrophobicity of the peptide to induce fusion and suggest that the oblique membrane insertion of the Aβ peptides and their fusogenic properties might potentiate toxicity. Elongation of the tilted peptides at their N-terminal end do not significantly modify their fusogenic properties. The Aβ-(22–42) and the Aβ-(12–42) peptides still induce the fusion of LUVs and SUVs as determined by lipid-mixing and core-mixing assays (Figs. 8–10) and by visible absorbance measurements (not shown). Since the Aβ-(13–28) peptide is not able to cause fusion, these data strongly suggest that the C-terminal end of the Aβ peptide is indeed responsible for the interaction and the destabilization of the lipid bilayer and for further fusion. Moreover, the tilted C-terminal peptide retains its fusogenic properties within the longer peptides, thus providing valuable clues toward the neurotoxic effect of the entire peptide. The decreased fusogenic capacity of the Aβ-(12–42) and Aβ-(22–42) peptides compared with that of the Aβ-(29–40) and the Aβ-(29–42) peptides, might be due to sterical hindrance created by the folding of the entire peptide. It has been reported that a change in the conformation of a protein could result in the exposure of the fusion peptide. At the pH of fusion, an essentially irreversible conformational change of influenza virus hemaglutinin results in the exposure of the N-terminal fusion peptide (37, 38). Experiments are currently performed to determine to what extent the structure of the entire Aβ peptide could be modified by the incubation conditions and to correlate those parameters with the fusogenic activity of the C-terminal domain of the Aβ peptide.

We further investigated the ability of the tilted amyloid peptides to modify the permeability of the SUVs by measuring the leakage of the encapsulated calcein from the vesicles, upon the addition of the peptides. The rate of increase of the calcein fluorescence intensity was taken as an index of the changes in vesicle permeability. There was release of calcein upon addition

of the Aβ-(29–40), Aβ-(29–42), Aβ-(22–42), and Aβ-(12–42) peptides. Thus, the amyloid peptides induce vesicle fusion with concomitant alteration of the bilayer permeability. On the contrary, the Aβ-(12–28) and the Aβ-(29–42) mutant peptides do not cause significant calcein release, suggesting an absence of efficient bilayer perturbation mediated by these peptides. Our results strongly suggest that the C-terminal end of the β-amyloid peptide is able to induce liposomal fusion through its deep insertion at a tilted angle into the lipid phase and that fusion. Data from fusion experiments, together with membrane perturbation of the liposomes, inducing calcein release out of the vesicles support the conclusion that fusion of liposomes induced by the amyloid peptides is accompanied by membrane leakage. Moreover, it has been proposed that membrane fusion, which takes place after insertion of the peptide into the membrane, is followed and amplified by the self-aggregation of peptide within the lipid phase, suggesting that peptide oligomerization might play an important role in the fusion induced by polypeptides (39, 40). In separate experiments, we have shown that the Aβ-(29–42) peptide aggregates more rapidly than the Aβ-(29–40) peptide in an aqueous buffer and forms amyloid-like fibrils.[2] This is in good agreement with the enhanced fusogenic properties of the Aβ-(29–42) peptide. We therefore propose that the C-terminal domain of the amyloid peptide is able to interact directly with a lipid bilayer, due to its obliquity and hydrophobicity, and to insert into the membrane. This interaction mechanism might account for the perturbation of cellular membranes by the amyloid peptide and for its toxicity toward a wide range of cells. In its soluble form, the amyloid peptide is toxic only at high concentrations, while the extensively aggregated peptide is not toxic. The Aβ peptide, either in its soluble form or when present in diffuse amyloid plaques, can reach high concentrations and be in the appropriate conformation to interact with a lipid membrane through its C-terminal domain. This might cause membrane perturbation and increase the susceptibility of the cell to further damages. According to this hypothesis, the amyloid peptide might be lethal to cells through its interaction with the neuronal plasma membrane, which in turn might activate one or more enzymatic or second messenger systems, and thus lead to cell death. In conclusion, the β-amyloid peptide is able to promote the fusion of phospholipids, causing modification of both the lipid structure and the bilayer permeability. Bilayer fusion, and thus insertion of the peptide into membrane might reflect the processes occurring during the interaction of amyloid peptide with neuronal cell membranes and thus it gives an insight into the molecular basis of the cytotoxicity of this potentially toxic peptide.

Acknowledgments—We thank H. Caster and J. Taveirne for excellent technical assistance.

[2] T. Pillot, M. Goethals, B. Vanloo, C. Talussot, R. Brasseur, J. Vandekerckhove, M. Rosseneu, and L. Lins, manuscript in preparation.

REFERENCES

1. Selkoe, D. J. (1994) *Curr. Opin. Neurobiol.* **4,** 708–716
2. Mattson, M. P. (1995) *Nat. Struct. Biol.* **2,** 926–928
3. Burdick, D., Soreghan, B., Kwon, M., Kosmoski, J., Knauer, M., Henschen, A., Yates, J., Cotman, C., and Glabe, C. (1992) *J. Biol. Chem.* **267,** 546–554
4. Hilbich, C., Kisters-Woike, B., Reed, J., Masters, C. L., and Beyreuther, K. (1991) *J. Mol. Biol.* **218,** 149–163
5. Jarrett, J. T., Berger, E. P., and Lansbury, P. T. (1993) *Biochemistry* **32,** 4693–4697
6. Lansbury, P. T., Costa, P. R., Griffiths, J. M., Simon, E. J., Auger, M., Halverson, K. J., Kocisko, D. A., Hendsch, Z. S., Ashburn, T. T., Spencer, R. G. S., Tidor, B., and Griffin, R. G. (1995) *Nat. Struct. Biol.* **2,** 990–998
7. Simmons, L. K., May, P. C., Tomaselli, K. J., Rydel, R. E., Fuson, K. S., Brigham, E. F., Wright, S., Lieberburg, I., Becker, G. W., Brems, D. N. (1993) *Mol. Pharmacol.* **15,** 373–379
8. Pike, C. J., Burdick, D., Walencewicz, A. J., Glabe, C. G., and Cotman, C. W. (1993) *J. Neurosci.* **13,** 1676–1687
9. Ueda, K., Fukui, Y., and Kageyama, H. (1994) *Brain Res.* **639,** 240–244
10. Arispe, N., Pollarde, H. B., and Rojas, E. (1993) *Proc. Natl. Acad. Sci. U. S. A.* **90,** 10573–10577
11. Arispe, N., Pollarde, H. B., and Rojas, E. (1993) *Proc. Natl. Acad. Sci. U. S. A.* **90,** 567–571
12. Weiss, J. H., Pike, C. J., and Cotman, C. W. (1994) *J. Neurochem.* **62,** 372–375
13. Mattson, M. P., Cheng, B., Davis, D., Bryant, K., Liederburg, I., and Rydel, R. E. (1992) *J. Neurosci.* **12,** 379–389
14. Schubert, D., Behl, C., Lesley, R., Brack, A., Dargusch, R., Sagara, Y., and Kimura, H. (1995) *Proc. Natl. Acad. Sci. U. S. A.* **92,** 1989–1993
15. Hensley, K., Carney, J. M., Mattson, M. P., Aksenova, M., Harris, M., Wu, J. F., Floyd, R. A., and Butterfield, D. A. (1994) *Proc. Natl. Acad. Sci. U. S. A.* **91,** 3270–3274
16. Brasseur, R. (1991) *J. Biol. Chem.* **266,** 16120–16127
17. Martin, I., Dubois, M. C., Defrise-Quertain, F., Saermark, T., Burny, A., Brasseur, R., and Ruysschaert, J. M. (1994) *J. Virol.* **68,** 1139–1148
18. Vonèche, V., Portetelle, D., Kettman, R., Willemms, L., Limbach, K., Paoletti, E., Ruysschaert, J. M., Burny, A., and Brasseur, R. (1992) *Proc. Natl. Acad. Sci. U. S. A.* **89,** 3810–3814
19. Zimmerberg, J., Vogel, S. S., and Chernomordik, L. V. (1993) *Annu. Rev. Biophys. Biomol. Struct.* **22,** 433–466
20. Horth, M., Lambrecht, B., Khim, M. C. L., Bex, F., Thiriard, C., Ruysschaert, J. M., Burny, A., and Brasseur, R. (1991) *EMBO J.* **10,** 2747–2755
21. Vancompernolle, K., Goethals, M., Huet, C., Louvard, D., and Vandekerckhove, J. (1992) *EMBO J.* **11,** 4739–4746
22. Brasseur, R., and Ruysschaert, J. M. (1986) *Biochem. J.* **238,** 1–11
23. Brasseur, R., Vanloo, B., Deleys, R., Lins, L., Labeur, C., Taveirne, J., Ruysschaert, J. M., and Rosseneu, M. (1993) *Biochim. Biophys. Acta* **1170,** 1–7
24. Brasseur, R., De Meutter, J., Vanloo, B., Goormaghtigh, E., Ruysschaert, J. M., Baert, J., and Rosseneu, M. (1991) *J. Lipid Res.* **32,** 1253–1264
25. Johnson, W. C., Jr. (1990) *Proteins Struct. Funct. Genet.* **7,** 205–214
26. Poduslo, S. E., and Norton, W. T. (1975) *Methods Enzymol.* **35,** 561–579
27. Rapaport, D., and Shai, Y. (1994) *J. Biol. Chem.* **269,** 15124–15131
28. Kendall, D. A., and MacDonald, R. C. (1982) *J. Biol. Chem.* **257,** 13892–13895
29. Bartlett, G. R. (1959) *J. Biol. Chem.* **234,** 466–468
30. Defrise-Quertain, F., Cabiaux, V., Vandenbranden, M., Wattiez, R., Falmagne, P., and Ruysschaert, J. M. (1989) *Biochemistry* **28,** 3406–3413
31. Morris, S. J., Bradley, D., Carter, C. G., Smith, P. D., and Blumenthal, R. (1988) *Spectroscopic Membrane Probes* (Loem, L. M., ed) Vol. 1, pp. 161–191, CRC Press, Boca Raton, FL
32. Moe, G. R., and Kaiser, E. T. (1985) *Biochemistry* **24,** 1971–1976
33. Mousli, M., Bronner, C., Bockaert, J., Rouot, B., and Landry, Y. (1990) *Trends Pharmacol. Sci.* **11,** 358–362
34. Song, D. L., Chang, D. G., HO, C. L., and Chang, C. H. (1993) *Eur. J. Pharmacol.* **247,** 283–288
35. Blumenthal, R., Henkart, M., and Steer, C. J. (1983) *J. Biol. Chem.* **258,** 3409–3415
36. Gasset, M., Onaderra, M., Thomas, P. G., and Gavilanes, J. G. (1990) *Biochem. J.* **265,** 815–822
37. Rafalski, M., Ortiz, A., Rockwell, A., van Ginkel, L. C., Lear, J. D., DeGrado, W. F., and Wilschut, J. (1991) *Biochemistry* **30,** 10211–10220
38. Doms, R. W., Helenius, A., and White, J. (1985) *J. Biol. Chem.* **260,** 2973–2981
39. Nieva, J. L., Nir, S., Muga, A., Goni, F. M., and Wilschut, J. (1994) *Biochemistry* **33,** 3201–3209
40. Muga, A., Neugebauer, W., Hirama, T., and Surewicz, W. K. (1994) *Biochemistry* **33,** 4444–4448